Very large gold and silver sputtering yields induced by keV to MeV energy Au_n clusters ($n=1-13$)

S. Bouneau,[1] A. Brunelle,[1,*] S. Della-Negra,[1] J. Depauw,[1] D. Jacquet,[1] Y. Le Beyec,[1] M. Pautrat,[1] M. Fallavier,[2] J. C. Poizat,[2] and H. H. Andersen[3]

[1]*Institut de Physique Nucléaire d'Orsay, UMR 8608, CNRS-IN2P3-Université Paris-Sud, 91406 Orsay Cedex, France*

[2]*Institut de Physique Nucléaire de Lyon, UMR 5822, CNRS-IN2P3-Université Claude Bernard, 43 Boulevard du 11 novembre 1918, 69622 Villeurbanne Cedex, France*

[3]*Niels Bohr Institute, Ørsted Laboratory, Universitetsparken 5, DK-2100 Copenhagen Ø, Denmark*

(Received 11 May 2001; revised manuscript received 6 November 2001; published 29 March 2002)

The total sputtering yields of gold and silver targets bombarded by Au_n ($n=1-13$) clusters have been measured over a broad range of incident energy per atom (from 20 keV/atom to 5 MeV/atom). Large nonlinear effects in the sputtering yields were observed. For silver targets, yield values as high as ~20 000 atoms per impact of Au_{13} at 1.2 MeV (92 keV/atom) were measured while only 45 atoms are emitted from the same target in the impact of single gold atoms at the same energy per atom. The sputtering yield variation with incident projectile energy per atom shows that maxima occur at ~250 keV/atom for a gold target and ~150 keV/atom for a silver target for projectiles with three or more atoms. In both cases the maxima of nuclear stopping power are at much larger energies per atom (700 keV for Au on Au and 550 keV for Au on Ag). Large surface deformations with craters and rims are observed by atomic force microscopy at the surface of cluster irradiated targets. Their number per unit area corresponds to the irradiation fluence and they are of approximately the same size, demonstrating that fluctuations between events are small.

DOI: 10.1103/PhysRevB.65.144106 PACS number(s): 79.20.Rf, 36.40.−c, 61.80.Lj, 68.49.Sf

I. INTRODUCTION

Polyatomic projectiles bombarding solids give rise to various effects: crater formation, material modifications, secondary emission with yields (ions, neutrals) that are much larger than if induced by the same number of constituents arriving individually. Usually called nonlinear, these effects were first observed more than 20 years ago in sputtering.[1,2] Earlier data were summarized and discussed shortly before the present measuring series started.[3] Recently the total sputtering yield of a gold target bombarded by Au_n ($n=1-5$) clusters was measured over a large incident energy range from 20–5000 keV per atom.[4] Sputtering yields as high as 3000 were found to be related to a dense energy deposition in the target through collisional nuclear processes. Unfortunately a few experimental yield values measured with Au_4 and Au_5 projectiles between 100 and 200 keV/atom were overestimated (due to the difficulty in measuring low intensities) and let us claim that the sputtering yield maxima were situated at a fixed total energy and not at the same energy per atom. The present paper is a continuation of the work of Ref. 4. Beams of large size gold clusters (up to Au_{13}) with higher intensities were used at both the Institut de Physique Nucléaire de Lyon (IPNL) and the Institut de Physique Nucléaire d'Orsay (IPNO) for systematic sputtering yield measurements from gold and silver surfaces.

II. EXPERIMENTAL

The gold cluster beams were mainly produced by a 2.5-MV Van de Graaff accelerator located at IPNL. This accelerator is equipped with a liquid metal ion source[5] installed in the high-voltage terminal of the machine and produces beams of gold clusters accelerated to total energies from 300 keV to 1.4 MeV.[6] A magnet at the exit of the accelerator is used to select the chosen Au_n^+ cluster, with n from 1 to 13. As the magnet deflects the heavy gold clusters at a very small angle only, a 6-m-long beam tube has to be used to sufficiently separate the desired cluster from the others. The maximum bending power of the magnet permits to deviate Au_{13}^+ ion beams having a total energy of 1.4 MeV at an angle of 3°. Above a total energy of 1.4 MeV, the cluster beams were delivered by the IPNO 15-MV tandem accelerator, which is also equipped with a liquid metal ion source in the high-voltage terminal.[7] Data from Ref. 4 obtained from the Aramis accelerator (located at the CSNSM laboratory at Orsay) have also been incorporated except the four points proved wrong by the present measuring series (see below).

The mass eroded from the target was measured with the quartz microbalance method.[8] A schematic view of the experimental setup is shown in Fig. 1. It has been completely rebuilt since the first experiments reported in Ref. 4 and only the already described quartz microbalance (model FTM5, Edwards, Manor Royal, Crawley, West Sussex, UK) is the same. Gold or silver is vapor deposited onto a standard quartz oscillator surface furnished by the microbalance manufacturer. The thickness of the deposited metal is 10^4 Å, which is thick enough to stop the projectiles, whatever their energy, in the metal far in front of the quartz itself but is still thin enough not to disturb the quartz oscillations. The cluster beam passes through a 2.7×2.7 mm^2 square aperture at the entrance of the experimental chamber. Its intensity is measured before each sputtering measurement with a Faraday cup located on the beam axis at the back of the chamber and equipped with secondary electron suppression. Upstream the Faraday cup, the movable quartz microbalance may be precisely positioned (±0.2 mm) on the beam axis for the sput-

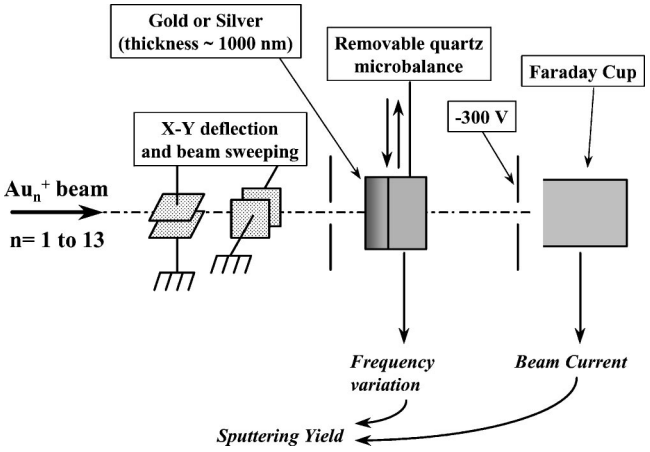

FIG. 1. Schematic view of the sputtering yield measurement setup.

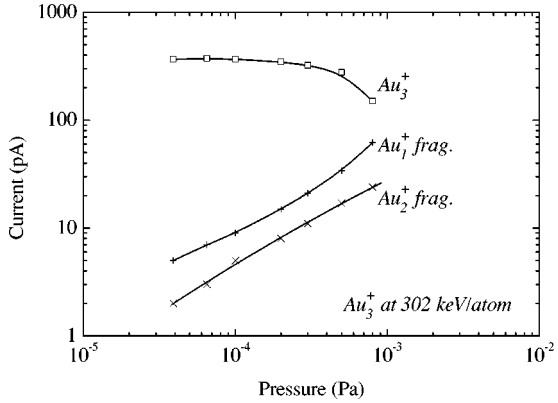

FIG. 2. Beam intensities measured with a Faraday cup for Au_3^+ ions and the fragment ions Au_2^+ and Au_1^+ at 302 keV/atom, as a function of residual gas pressure. The solid lines are guides for the eye.

tering yield measurements. Because of the rapid decrease of the quartz gauge sensitivity with increasing distance between its center and the beam axis (although the quartz diameter is 8 mm we have measured that 98% of its sensitive surface is situated within a 3 mm diameter; see also Ref. 9), it is very important to have both a precise and reproducible positioning of the quartz holder on the beam axis and a beam homogeneously irradiating the surface. The distance between the beam entrance aperture and the quartz is only 25 mm to ensure that possible misalignment of the beam gives rise to a negligible beam displacement on the quartz surface. It is possible at the IPNL Van de Graaff accelerator to rapidly sweep the beam horizontally and vertically with two sets of high-voltage deflection plates located ~50 cm in front of the aperture to guarantee an homogeneous irradiation of the target whatever the beam profile. The beam currents varied under these conditions from several nanoamperes for Au_1 to 10 pA for Au_{13}. The minimum current accepted for the present experiments was 5 pA, as lower currents could not be measured reliably. Comparisons between experimental points measured with the same beam at different beam currents revealed that the intensity was underestimated by 20–40 % below 5 pA, leading to a systematic overestimation of the sputtering yields for some experimental points in Ref. 4 (only four points out of 43). These experimental points (Au_4 at 100 and 187.5 keV/atom and Au_5 at 100 and 150 keV/atom) have been remeasured at the IPNL Van de Graaff accelerator in the present experiment.

The residual gas pressure in the experimental chamber and in the upstream beam line was always smaller than 10^{-4} Pa. The deflection plates shown in Fig. 1 were used to investigate breakup and charge exchange of the clusters through scattering on residual gas molecules during transmission through the 6-m beam tube. For that purpose a small air leak was introduced close to the entrance of the experimental chamber. An example is shown in Fig. 2, where the currents of Au_3^+ ions and the fragments Au_1^+ and Au_2^+ are plotted as a function of gas pressure between 4×10^{-5} and 8×10^{-4} Pa. A negligible fraction of less than 4% of the Au_3^+ ions was fragmented below 10^{-4} Pa. Therefore the residual gas pressure must be maintained below 10^{-4} Pa to avoid fragmentation. To test the possibility of neutralization, a sputtering yield measurement was performed during deflection of the charged beam for a time duration ten times larger than otherwise used to perform a measurement. No frequency variation of the quartz microbalance was observed during that test experiment.

Our data contain measurements made with the old[4] and the present setup and no systematic differences may be discerned. Within the experimental errors, estimated to be lower than 15%, our data are in agreement with previously published ones, obtained with gold,[10] lead,[2] and bismuth[11] projectiles, respectively, onto gold targets.

Gold was first chosen in Ref. 4 in order to maximize the expected nonlinear effect and in order to avoid problems of target contamination by the incoming beam. The second target chosen in the present experiments was silver for which the ratio of the nuclear stopping power over the surface binding energy was roughly the same as for gold within the energy range studied. This ratio is an important parameter in both the linear cascade theory[12] and spike models.[13]

III. RESULTS AND DISCUSSION

A. Sputtering yields as a function of projectile size and energy

Tables I and II show the experimental sputtering yields divided by the number of constituents of the Au_n^+ ($n=1-13$) cluster projectiles for gold and silver targets, respectively. These values are presented in Fig. 3 as a function of the projectile energy per atom and without the error bars for clarity of the figure. This figure directly shows that sputtering yields per atom increase more rapidly at a given velocity than the number of constituents in the projectile, which means that nonlinear enhancements of the sputtering yield are induced by the impact of polyatomic projectiles (otherwise all the curves would have been on top of each other). The maximum values obtained in the present experiments are 19 550 ($\pm$1200) silver atoms sputtered per impact of 1200-keV Au_{13}, and 14 300 ($\pm$1300) gold atoms per impact of 1400-keV Au_{13}. These sputtering yields are the highest ever obtained on metals. The silver sputtering yields are,

TABLE I. Gold sputtering yields per atom measured for different gold cluster projectiles.

Projectile	Incident energy per atom (keV/atom)	Sputtering yield per atom Y/n	Projectile	Incident energy per atom (keV/atom)	Sputtering yield per atom Y/n
Au_1	33	32±2	Au_5	20	123±16
	50	34.5±4		60	320±32
	75	49±6		100	406±28
	100	54±5		140	477±42
	200	62±6.5		200	543±40
	350	78±6		224	555±136
	700	79±7		280	556±42
	1400	66±5.5		299	482±55
	2800	44±3.5		446	407±52
Au_2	20	50±4		500	422±73
	33	55±5.5		1000	398±32
	100	142±14.5		1800	187±20
	130	152±15	Au_7	43	358±77
	200	162±18		71	392±29
	350	200±22.5		100	529±41
	700	150±18		143	710±82
	1400	101±12		200	719±55
	5000	63±5	Au_9	33	348±21
Au_3	20	79±5.5		55	370±38
	33	101±9.7		78	572±97
	100	235±25		111	830±80
	133	261±26		155	943±103
	167	322±18	Au_{11}	45	400±39
	200	303±17		64	554±43
	350	289±15		91	850±62
	468	275±17		127	1140±160
	700	248±16	Au_{13}	54	544±49
	3000	100±6		77	920±90
Au_4	20	97±8		107	1100±102
	25	133±11			
	75	281±30			
	125	319±29			
	175	397±31			
	250	418±39			
	351	396±57			
	500	329±34			

for given cluster size and velocity, always larger than those of gold. Although it has been mentioned above that the ratio of the stopping power over the surface binding energy is the same for gold and silver, it seems that the sputtering yields increase with decreasing surface binding energy (3.78 eV and 3.04 eV for gold and silver, respectively).

For $n=1$, yield variations as a function of energy present a maximum at roughly the same energy as the maximum of the nuclear stopping power at the surface, ~700 keV and ~550 keV for gold onto gold and silver targets, respectively (calculated with the SRIM2000 code).[14] For n values between 2 and 5, the maxima of the yield curves shift gradually towards lower velocities to reach values of ~250 keV/atom for gold and ~150 keV/atom for silver, which are smaller than for the maximum of nuclear stopping power as given above. For n larger than 5 it was not possible to obtain experimental values at sufficiently high energies per atom to reach the expected maximum yields, because of the limited energy range of the IPNL Van de Graaff accelerator as well as the limited beam intensity at the IPNO Tandem accelerator.

In order to highlight the strong increase of the experimental yields with increasing projectile size, Fig. 4 shows the variations of Y/n^2 as a function of the energy per atom. It is clear from this figure that above $n=2$ (gold) and 3 (silver), all the sputtering yields roughly scale with n^2 and that the yields increase more rapidly than n^2 between $n=1$ and 2 and between $n=2$ and 3.

Large enhancements of secondary ion emission yields were previously measured with gold clusters in the same incident energy range but with different types of materials

TABLE II. Silver sputtering yields per atom measured for different gold cluster projectiles.

Projectile	Incident energy per atom (keV/atom)	Sputtering yield per atom Y/n	Projectile	Incident energy per atom (keV/atom)	Sputtering yield per atom Y/n
Au_1	33	30±2		1000	183±14
	100	51±3		1800	104±11.5
	300	47±3	Au_7	43	466±28
	600	47±5		71	677±43
Au_2	80	172±7.5		93	828±73
	150	173±9.6		100	846±50
	200	173±5.2		110	904±93
	375	121±2.7		128	800±47
	710	71±2.5		130	848±70
Au_3	50	241±13.5		171	890±35
	93	343±20		200	895±60
	100	400±22	Au_9	33	504±30
	150	408±26		55	718±47
	167	402±24		72	963±80
	217	383±24		78	896±51
	300	254±16		100	1023±72
	400	221±10		133	1108±67
	467	198±12		156	1260±73
	600	142±12	Au_{11}	27	497±56
	1000	98±6		45	700±50
	3000	46±2.5		59	1010±77
Au_5	30	274±17		82.7	1210±152
	60	488±25		100	1280±64
	100	660±41		127	1560±90
	130	629±35	Au_{13}	38	731±50
	182	613±38		50	1000±73
	240	572±29		69	1300±156
	280	466±30		92	1500±95

(CsI, organic materials).[15] The highest ion emission yields were also observed at much lower energy per atom than the expected maxima of the nuclear stopping. This behavior seems to be a general trend in large cluster induced secondary emission.

B. Target surface modifications and volume ejected

A Au_{11} cluster projectile having a total energy of 1.4 MeV (127 keV atom) close to the maximum of the sputtering yield ejects 12 500±1700 gold atoms from a gold target. This number corresponds to a volume of $\sim 2.1\times 10^5$ Å^3 (the density of gold is 19.3 g cm^{-3}), which could be a cone with a depth $h=93$ Å and base diameter $D=h$ or a cylinder with a monolayer height of 2.5 Å and a surface diameter of 330 Å. Atomic force microscopy (AFM) of a gold surface irradiated with these 127 keV/atom Au_{11} clusters was performed. The fluence was moderate, 1.6×10^{10} clusters cm^{-2}, in order to have a negligible probability of crater overlapping. A perspective view of such an AFM image is shown in Fig. 5. The observed surface deformation has the shape of a crater surrounded by a rim. From the *AB* section in Fig. 5, one can estimate a crater diameter of 250 Å. It is larger than that deduced from the sputtering yield but it is seen that a fraction of the matter removed from the crater is redeposited or pushed up around it. The crater depth cannot be deduced with any certainty from an AFM measurement but one can nevertheless deduce an estimate of the cone depth from both the sputtered volume and the above crater diameter (Fig. 5). The obtained value of $h\sim 13$ Å is intermediate between the two extreme cases mentioned above. A rough estimate of the number of craters per unit surface is in agreement within 20% with the irradiation fluence and as it may further be seen that all craters have very similar dimensions (445 ±60 Å), fluctuations in the yield cannot play a substantial role.

C. Sputtering yields as a function of nuclear stopping power

Figure 6 shows total sputtering yields (not divided by n) as a function of the total nuclear stopping power at the surface (for the incident projectile energy per atom E/n). The electronic energy loss is not considered despite the fact that it amounts to more than 20% of the total energy loss at the highest energies investigated. This is justified by recent experiments by Assman *et al.*,[16] who, at much higher energies

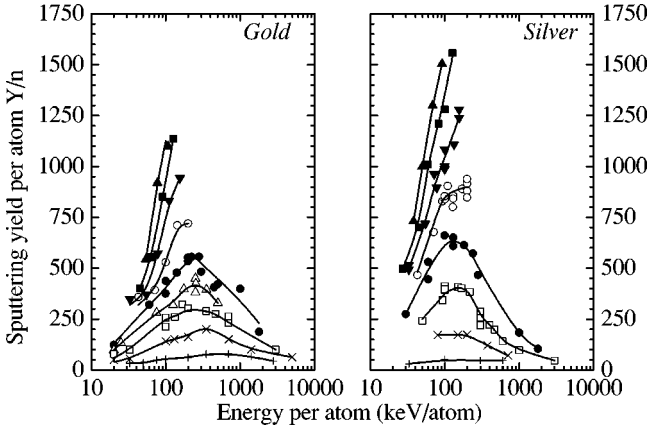

FIG. 3. Gold and silver sputtering yields per atom Y/n, as a function of the energy per atom of the Au_n $(n=1-13)$ cluster projectiles. The solid lines are guides for the eye. Symbols used correspond to following values of n: + 1, × 2, □ 3, △ 4, ● 5, ○ 7, ▼ 9, ■ 11, ▲ 13.

where electronic stopping is totally dominating, found very small sputtering yields for metals. The stopping power, easy to calculate using SRIM tables, has been used. It is assumed that the nuclear stopping power of a Au_n^+ cluster is n times the nuclear stopping power of a single Au^+ ion at the same velocity. For a n-constituent cluster projectile having a total energy E the notation is the following:

$$\left(\frac{dE}{dx}(n,E)\right)_{\text{nuc}} = n\left(\frac{dE}{dx}(1,E/n)\right)_{\text{nuc}}. \qquad (1)$$

This assumption is in agreement with theoretical estimates[17] is and supported by recent projected-range measurements. Au_n $(n=1-3)$ clusters at 10–40 keV/atom were implanted in Si, Al, and Cu. The Si target was amorphous, the metal targets fine grained polycrystalline. Further, one set of measurements was performed with 44.3-keV/atom Au_1 and Au_7 in Si (amorphous). These range distributions were in all cases identical within their measuring accuracy.[18]

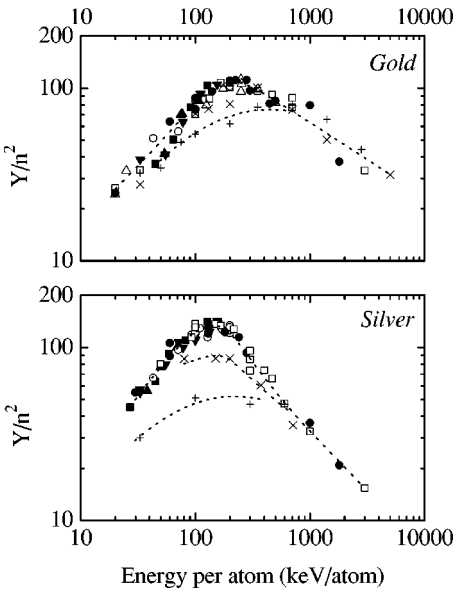

FIG. 4. Gold and silver sputtering yields divided by n^2, as a function of the energy per atom of the Au_n $(n=1-13)$ cluster projectiles. The dashed lines are guides for the eye. Symbols as same as in Fig. 3.

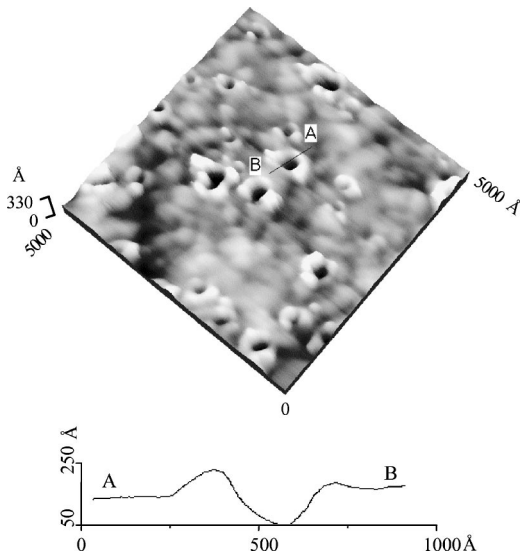

FIG. 5. Atomic force microscope image (perspective view) of a gold surface (area $5000\times5000\,\text{Å}^2$) irradiated with 1.61×10^{10}-cm^{-2} Au_{11} ions having an energy of 1.4 MeV (127 keV/atom).

For each cluster projectile size shown in Fig. 6 the total sputtering yields follow a line of slope 2 on a log-log presentation, as long as the energy remains below that of the yield maxima, indicating that in this region the yields are proportional to the square of the total nuclear stopping. Fig-

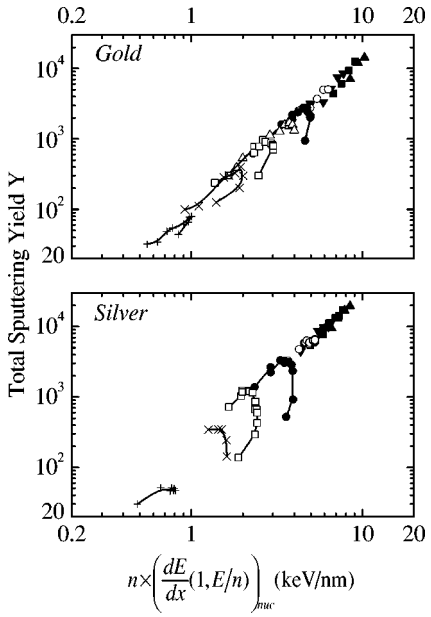

FIG. 6. Gold and silver total sputtering yields Y, as a function of the tabulated (Ref. 14) projectile nuclear stopping power $n(dE/dx(1,E/n))_{\text{nuc}}$, and for Au_n $(n=1-13)$ cluster projectiles. Symbols correspond to Fig. 3. Solid lines are guides for the eye.

ure 6 also clearly shows that there is a region where the stopping still increases with energy, while the yields decrease with increasing energy. In this region the proportionality to $[dE/dx(n,E)]^2_{\mathrm{nuc}}$ breaks down. These ''hooks'' in the curves demonstrate that there is no simple relation between the sputtering yields and the nuclear stopping power at the surface. Similar curves have been observed in the electronic stopping-power regime.[19] An effect of the projectile velocity appears, as slow projectiles induce larger yields than fast projectiles having the same value of $[dE/dx(n,E)]_{\mathrm{nuc}}$.

D. Comparison with molecular-dynamic simulations

Recent molecular-dynamic (MD) simulations have been performed for gold sputtered under gold cluster bombardment. In Refs. 20 and 21 gold clusters with energies per atom smaller than (or equal to) 16 keV/atom were used. The authors predict huge sputtering yields, depending strongly on cluster size and energy. The MD simulation pictures show that craters and crater rims are formed, as observed in the present work in AFM pictures. The simulations also demonstrate that a substantial fraction of the atoms excavated from the crater is redeposited to form a rim and that large clusters (chunks) are preferentially emitted from the craters' rims. The authors also found a strong correlation between the crater size and the sputtering yield.

In Ref. 22 the simulations of Au_5 cluster impacts are presented with a total energy of 800 keV. The authors predicted that a substantial fraction of the simulated impacts produced very little sputtering, while some individual sputtering events producing very large numbers of sputtered atoms contributed decisively to the total sputtering yield. The prediction of ''superevents'' is in contradiction to the present AFM measurements (Fig. 5) in which no substantial fluctuation in the crater size is observed, and where the density of craters roughly agrees with the impacting cluster fluence.

MD simulations accounting for electronic sputtering are presented, among others, in Refs. 23–25. This work describes the energy relaxation mechanisms in solids independently of the energy-deposition processes. The authors obtained a relation between the sputtering yield and a fraction of the electronically deposited energy, going into nonradiative deexcitations and contributing to sputtering. They concluded that the sputtering yield has a quadratic dependence on small stopping powers $[Y \propto (dE/dx)_{\mathrm{ele}}{}^2]$ and a linear dependence on large stopping powers $[Y \propto (dE/dx)_{\mathrm{ele}}]$. The simulations were performed for a constant and given track diameter. In the region where the yield was found to be proportional to (dE/dx), it was also found, for fixed (dE/dx), to be proportional to the track diameter ρ. Unfortunately we do not have within this picture an independent way to estimate ρ and to tell in which region we are situated. To fit our quadratic dependence on n, we may, therefore, be in the region where the yields are directly proportional to $(dE/dx)^2$, or in the (dE/dx) region but with ρ proportional to n. A proportionality to n is certainly too strong a dependence of ρ on n, but some increase is not unrealistic. When a cluster impinges on a target, the first part of the cascades from the individual atoms will develop independently, and there will not be total overlap meaning that the total radius will grow with increasing n. In such a picture the developed energy-deposition plume is not cylindrical, but this is not either the case for the individual cascades. The cylindrical-spike model is in any case an approximation. A growth of ρ proportional to n sounds, however, unrealistic, as that would imply that the deposited-energy density would in fact decrease with increasing n. Comparison with the trends found in the simulations are thus difficult and track diameters may not even be extracted through a fitting procedure.

E. Comparison with thermal spike models

The thermal spike theory of Sigmund and Claussen[13] was discussed in Ref. 4. In their model the sputtering yield is assumed to be the sum of the well-established linear collision cascade yield[12] plus a contribution from a thermal spike induced surface evaporation. The calculated linear yield (which contains no free parameters) fits existing yield data for Au on Au and Ag very well at energies far above and below the maximum of the nuclear stopping power but underestimates the data in the energy region corresponding to the maxima of the sputtering yield and of nuclear stopping power.[3,10] For lighter particles and/or targets the linear yield is predicted very well indeed over the entire energy region.[26] The thermal spike in the model is assumed to be cylindrical, perpendicular to the surface and infinitely long in the version of the theory that we apply here. During evaporation from the surface, the spike is cooled through heat conduction to the sides and the yield is obtained through an integration of the temperature-dependent evaporation over time. The result is that the sputtering yield should be proportional to the square of the linear sputtering yield (and hence to the square of the nuclear stopping) times a Bolztmann factor. The temperature in the latter is given by the average deposited energy per atom in the initial spike. Sigmund and Claussen, in their original paper, assumed this initial spike radius ρ_0 to be the mean square lateral straggling of the collision cascade, and obtained a reasonable fit to the data of Johar and Thompson.[11] Recently Sigmund[27] calculated initial track radii for a broad energy range and made comparisons to the radii we extracted in our previous publication.[4] As he did not consider a dependence of ρ_0 on n, we preferred also in the present context to extract ρ_0 using the theory,[13] rather than presenting calculated absolute yield curves compared to the measured ones. We first note that the n^2-proportional region implies a constant value of the Bolztmann factor. To obtain that, ρ_0 must be proportional to $n^{1/2}$. This is more plausible than the n proportionality mentioned above in connection with the discussion of an aspect of the computer simulations, but still it is too fast: there must be some, although not complete, overlap of the individual cascades. With regard to the energy dependence of ρ_0, we find our extracted values to grow approximately as $E^{1/6}$. This is slower than predicted by Sigmund.[27] But note that if ρ_0 increases with energy, the maximum of the yields must, due to the following decrease of the Bolztmann factor, appear at lower energies than that of the maximum in nuclear stopping. We conclude that although

some features of our results are well explained within the Sigmund-Claussen theory,[13] other aspects are difficult to reconcile with their model.

Other analytical theories are due to Bitensky,[28] Urbassek and Michl,[29] and Jakas and Bringa.[30] Bitensky treats the influence of fluctuations on the onset of the spike. His theory is thus not relevant for large-cluster impacts, where we have full n^2 scaling and each event gives rise to a crater. Urbassek and Michl treat a gas flow model that may not be ruled on the basis of the present measurements. The model does, however, lead to a rather narrow angular distribution of the sputtered material, which is in disagreement with recent results of Andersen, Johansen, and Touboltsev.[31] Finally, Jakas and Bringa's model[30] is in its starting point close to that of Sigmund and Claussen[13] in the sense that they start with a semi-infinite cylinder with a constant high temperature proportional to dE/dx. As suggested by the simulations of Bringa and co-workers[23–25] (in an extended version of the standard thermal spike theory of sputtering[13] including the transport of mass, a realistic heat capacity, and the heat of melting), at large deposited energies the thermal pressure in the hot core of the spike gives rise to an elastic wave, which expands laterally and cools the spike, lowering the sputtering yield. Jakas and Bringa cannot reproduce the dE/dx proportional results of Bringa and co-workers, but find a faster rise of the yield with dE/dx. Nevertheless, the Jakas and Bringa cooling mechanism might explain why the experimental sputtering yield maxima are reached at an energy per atom lower than for the maximum nuclear stopping power.

IV. CONCLUSION AND OUTLOOK

Following a series of previous measurements[4] on sputtering of Au targets with a limited size range of Au_n clusters $(n=1-5)$, measurements over a broad projectile energy interval have been pursued with large cluster sizes (up to $n=13$) and with both gold and silver targets. It is observed that for clusters with $n \geqslant 3$ all the sputtering yields are proportional to the square of the number of constituents and have their maxima at the same energy per atom, which is much smaller than the energy of the maximum of the nuclear stopping power.

The sputtering yield values that have been measured are the largest ever observed with metallic targets and could not be predicted by theoretical models in the energy range investigated. The experimental data set presented here, which is now more complete, is hoped to be useful for future comparisons with both spike models and MD simulations.

In the future, the size of the projectiles could be increased to a point where an important fraction of the energy is released through sputtering processes, and it would also be interesting to explore the sputtering limit in terms of ejected matter per impact of a large object. Beams of gold clusters containing up to 100 atoms were already accelerated to several tens of keV/atom. Large intact clusters and/or chunks of matter will certainly be emitted in the bombardment of solids with these beams. This probably occurs already with the beams of Au_n^+ used in this work and cluster emission should be considered in models. Measurements of the mass distribution of the sputtered species with a postionization method should thus be performed.

ACKNOWLEDGMENTS

Technical support during the experiments by Y. Champelovier (IPNL Van de Graaff accelerator) and by the IPN-Orsay Tandem accelerator group is gratefully acknowledged. We also thank J. C. Girard from the University of Poitiers who performed the AFM measurements. One of us (H.H.A.) thanks the Danish National Science Research Council (SNF) for grants that allowed his participation in the experiments.

*Corresponding author. Email address: brunelle@ipno.in2p3.fr

[1] H. H. Andersen and H. L. Bay, J. Appl. Phys. **45**, 953 (1974).
[2] H. H. Andersen and H. L. Bay, J. Appl. Phys. **46**, 2416 (1975).
[3] H. H. Andersen, Mat. Fys. Medd. K. Dan. Vidensk. Selsk. **43**, 127 (1993).
[4] H. H. Andersen, A. Brunelle, S. Della-Negra, J. Depauw, D. Jacquet, Y. Le Beyec, J. Chaumont, and H. Bernas, Phys. Rev. Lett. **80**, 5433 (1998).
[5] M. Benguerba, A. Brunelle, S. Della-Negra, J. Depauw, H. Joret, Y. Le Beyec, M. G. Blain, E. A. Schweikert, G. Ben Assayag, and P. Sudraud, Nucl. Instrum. Methods Phys. Res. B **62**, 8 (1991).
[6] M. Fallavier, Y. Champelovier, M. Ferrari, R. Kirsch, J. C. Poizat, J. Remillieux, J. P. Thomas, B. Canut, S. M. M. Ramos, P. Thévenard, S. Della-Negra, J. P. Mouffron, and P. Nicol, Eur. Phys. J. D **9**, 529 (1999).
[7] S. Della-Negra, A. Brunelle, Y. Le Beyec, J. M. Curaudeau, J. P. Mouffron, B. Waast, P. Håkansson, B. U. R. Sundqvist, and E. S. Parilis, Nucl. Instrum. Methods Phys. Res. B **74**, 453 (1993).
[8] H. H. Andersen and H. L. Bay, Radiat. Eff. **13**, 67 (1972).
[9] A. Oliva-Florio, R. A. Baragiola, M. M. Jakas, E. V. Alonso, and J. Ferron, Phys. Rev. B **35**, 2198 (1987).
[10] H. L. Bay, H. H. Andersen, W. O. Hofer, and O. Nielsen, Nucl. Instrum. Methods **132**, 301 (1976).
[11] S. S. Johar and D. A. Thompson, Surf. Sci. **90**, 319 (1979).
[12] P. Sigmund, Phys. Rev. **184**, 383 (1969); **187**, 768 (1969).
[13] P. Sigmund and C. Claussen, J. Appl. Phys. **52**, 990 (1981).
[14] J. F. Ziegler, J. P. Biersack, and H. Littmark, *The Stopping and Ranges of Ions in Solids* (Pergamon, New York, 1985).
[15] A. Brunelle, S. Della-Negra, J. Depauw, D. Jacquet, Y. Le Beyec, M. Pautrat, K. Baudin, and H. H. Andersen, Phys. Rev. A **63**, 022902 (2001).
[16] W. Assman *et al.* (unpublished).
[17] V. I. Shulga and P. Sigmund, Nucl. Instrum. Methods Phys. Res. B **47**, 236 (1990).
[18] H. H. Andersen, A. Johansen, M. Olsen, and V. Tuboltsev (unpublished).
[19] P. Dück, W. Treu, H. Fröhlich, W. Galster, and H. Voit, Surf. Sci. **95**, 603 (1980).
[20] Th. J. Colla and H. M. Urbassek, Nucl. Instrum. Methods Phys. Res. B **164-165**, 687 (2000).
[21] Th. J. Colla, R. Aderjan, R. Kissel, and H. M. Urbassek, Phys. Rev. B **62**, 8487 (2000).

[22] M. H. Shapiro and T. A. Tombrello, Nucl. Instrum. Methods Phys. Res. B **152**, 221 (1999).
[23] E. M. Bringa and R. E. Johnson, Nucl. Instrum. Methods Phys. Res. B **143**, 513 (1998).
[24] E. M. Bringa, R. E. Johnson, and L. Dutkiewicz, Nucl. Instrum. Methods Phys. Res. B **152**, 267 (1999).
[25] E. M. Bringa, M. M. Jakas, and R. E. Johnson, Nucl. Instrum. Methods Phys. Res. B **164-165**, 762 (2000).
[26] H. H. Andersen and H. L. Bay, in *Sputtering by Particle Bombardment I*, edited by R. Behrisch (Springer-Verlag, Berlin, 1981), Vol. 47, p. 145.
[27] P. Sigmund, Nucl. Instrum. Methods Phys. Res. B **164-165**, 401 (2000).
[28] I. S. Bitensky, Nucl. Instrum. Methods Phys. Res. B **83**, 110 (1993).
[29] H. M. Urbassek and J. Michl, Nucl. Instrum. Methods Phys. Res. B **22**, 480 (1987).
[30] M. M. Jakas and E. M. Bringa, Phys. Rev. B **62**, 824 (2000).
[31] H. H. Andersen, A. Johansen, and V. S. Touboltsev, Nucl. Instrum. Methods Phys. Res. B **164-165**, 727 (2000).